International Journal of Applied Mechanics
Vol. 6, No. 6 (2014) 1450069 (20 pages)

DOI: 10.1142/S1758825114500690

A REDUCED ORDER MODEL BASED ON BLOCK ARNOLDI METHOD FOR AEROELASTIC SYSTEM

QIANG ZHOU, GANG CHEN* and YUEMING LI

*State Key Laboratory for Strength and Vibration
of Mechanical Structures, School of Aerospace
Xi'an Jiaotong University, Xi'an 710049, P. R. China*
*aachengang@mail.xjtu.edu.cn

Received 16 January 2014
Revised 6 September 2014
Accepted 16 September 2014
Published 17 November 2014

A reduced-order model (ROM) based on block Arnoldi algorithm to quickly predict flutter boundary of aeroelastic system is investigated. First, a mass–damper–spring dynamic system is tested, which shows that the low dimension system produced by the block Arnoldi method can keep a good dynamic property with the original system in low and high frequencies. Then a two-degree of freedom transonic nonlinear aerofoil aeroelastic system is used to validate the suitability of the block Arnoldi method in flutter prediction analysis. In the aerofoil case, the ROM based on a linearized model is obtained through a high-fidelity nonlinear computational fluid dynamics (CFD) calculation. The order of the reduced model is only 8 while it still has nearly the same accuracy as the full 9600-order model. Compared with the proper orthogonal decomposition (POD) method, the results show that, without snapshots the block Arnoldi/ROM has a unique superiority by maintaining the system stability aspect. The flutter boundary of the aeroelastic system predicted by the block Arnoldi/ROM agrees well with the CFD and reference results. The Arnoldi/ROM provides an efficient and convenient tool to quick analyze the system stability of nonlinear transonic aeroelastic systems.

Keywords: Aeroelasticity; reduced-order model; block Arnoldi algorithm; proper orthogonal decomposition.

1. Introduction

In many science and engineering fields, like fluid or structural mechanics [Kerschen *et al.*, 2005], electric circuit design, especially in fluid-structure coupling systems [Griffith *et al.*, 2009; Tan *et al.*, 2009; Lantz *et al.*, 2011] and other coupling systems [Li *et al.*, 2012; Xu *et al.*, 2014], the simulation time of large systems is still too high. What's more, some large-scale dynamical systems need to be optimized or controlled. These systems are computationally expensive due to their large orders [Yue and Meerbergen, 2013]. Large-scale dynamical systems often arise from the discretization of partial differential equations (PDEs). To reduce the simulation cost and storage requirement, reduced-order models (ROMs) are needed to develop a simplified mathematical model that can captures the dominant dynamic of the original system. In structural dynamics field, eigenvalue analysis [Bui and Nguyen, 2011] and then mode superposition method are widely used in industry, in which a limited number of free vibration modes of the structure is used to represent the displacement pattern. However, there are some important points to note on the expansion procedures used in practice. For example, the computation of eigenvectors for large systems is very expensive and time consuming. Besselink *et al.* [2013] reviewed and compared popular model reduction techniques in the structural dynamics fields, including mode displacement methods, Krylov subspace based model order reduction and balanced truncation. He also discussed the differences and similarities between these methods. As one of the most popular ROMs, proper orthogonal decomposition (POD) [Liang *et al.*, 2002] method was used to analyze the nonlinear vibrations of cylindrical shells with high efficiency [Amabili *et al.*, 2003]. Steindl and Troger [2001] compared the POD and nonlinear inertial manifold methods of their efficiency to reduce large amplitude oscillations of fluid conveying tube system. ROMs were successfully applied in structural–acoustic simulation [Kergourlay *et al.*, 2001] and optimization [Puri and Morrey, 2011] in recent years. Rumpler *et al.* [2014] extented the Padé-based reconstruction to the model reduction of poroelastic domains in poro-acoustic problems with good computational efficiency.

ROMs were also successfully applied in some coupling systems. Batra *et al.* [2008] presented a unified approach to derive ROMs for microelectromechanical clamped rectangular and circular plates system incorporating the Casimir force. Recently, ROMs are also implemented in multi-scale modeling [Xu *et al.*, 2014]. In fluid-structure coupling field, especially for aeroelastic problems, the coupling between the nonlinear aerodynamic loading and structural properties can lead to instability that may cause important damage or failure to structures. The prediction of aeroelastic instability in the transonic regime plays a very important role in the definition of the flight envelope for many high-performance aircrafts. With the development of computational capability, the aeroelastic computation based on CFD/CSD coupling methods can accurately predicted the nonlinear behaviors of full aircrafts in the subsonic, transonic and supersonic regimes. However, a typical CFD model, which can have 10^4 to 10^7 or more higher degrees of freedom (DOFs). Due to the large DOFs and extensive computational cost, it is unrealistic for engineering routine analysis and flexible wing optimization. So a high-fidelity nonlinear low order aerodynamic state space model is expected for rapid aeroelastic response analysis and flutter suppression control law design. In order to tackle this computational cost issue, ROMs methods have been proposed in the aeroelasticity community since last decade [Lucia *et al.*, 2004]. ROMs are very convenient to be used in conceptual design, control [Chen *et al.*, 2010, 2011; 2014], and data-driven systems.

Different approaches for reduced-order modeling and their applicability to various problems in computational physics were discussed by Lucia *et al.* [2004] including methods based on Volterra series representations, the POD, and harmonic balance. Most aeroelastic phenomena such as flutter and gust response can be dealt with these ROMs based on the dynamically linearized equation [Amsallem, 2010; Da Ronch *et al.*, 2012]. Among these approaches, the POD method is perhaps the most popular, which was widely used in many aeroelastic and structural dynamics problems [Amabili *et al.*, 2003; Chen *et al.*, 2010], such as the CFD-based aeroelastic analysis of a transport aircraft model and complete fighter configurations [Amsallem, 2010]. But the POD basis vectors must be obtained from the calculated snapshots of the system. Sometimes the snapshots cannot cover all the system information, and the ROMs produced by the POD basis may be different if the selected snapshots are different. POD-based models are sensitive to the choice of snapshots produced by sample frequencies or impulse time simulation. That implies that the accuracy of the POD/ROM maybe depend on the calculated snapshots [Willcox *et al.*, 2002]. It is not a good news for engineers.

Different from the data-driven POD method, the block Arnoldi algorithm can be used to generate orthonormal basis vectors in block Krylov subspace which is independent of snapshots data. Willcox *et al.* [2002] used the frequency domain Arnoldi-based method to construct ROMs for turbomachinery. The authors found that Arnoldi-based models are much cheaper to calculate than those constructed using POD basis vectors. Florea *et al.* [2000] used an alternative Arnoldi–Ritz vectors method to construct aeroelastic ROMs for unsteady transonic potential flow and predicted flutter boundaries of different aerofoils at several different Mach numbers. Arnoldi method can generate guaranteed stable and passive ROMs while Arnoldi vectors match only half the number of moments as the Pade approximation [Silveira *et al.*, 1999]. The above-mentioned Arnoldi methods are based on Krylov subspace and widely used in single-input single-output (SISO) system. It is not convenient for multi-input multi-output (MIMO) system.

For a MIMO aeroelastic system, a block approach based on block Krylov subspace is required. The block Arnoldi method generates orthonormal basis vectors from rth order block Krylov subspace. Only the matrices of the system's state-space equations are required to construct a ROM, so that it preserves system definiteness and stability. In this paper, we propose a ROM method based on the block Arnoldi method for nonlinear aeroelastic systems, which is compare with the POD method. The rest of this paper is organized as follows. The dynamic linearization of nonlinear aeroelastic equations and ROMs including block Arnoldi and POD method are described in Sec. 2. Some simulation cases include Mass–Damper–Spring system and NACA0012 aeroelastic system in transonic flow are described thoroughly in Sec. 3.

2. Reduced-Order Modeling for Dynamic Linearized Aeroelastic System

2.1. *The dynamic linearization of nonlinear aeroelastic equations*

The linearization method described here is based on a high-fidelity, CFD-based, nonlinear coupled aeroelastic model using an ALE non-dimensional conservative form of the Euler equations, which is written as follows [Amsallem, 2010]:

$$(\mathbf{A}(\mathbf{u})\mathbf{w})_{,\tau} + \mathbf{F}(\mathbf{w}, \mathbf{u}, \mathbf{v}) = \mathbf{0}_{N_f} \tag{1}$$

$$\mathbf{M}\dot{\mathbf{v}} + \mathbf{f}^{\text{int}}(\mathbf{u}, \mathbf{v}) = \mathbf{f}^{\text{ext}}(\mathbf{u}, \mathbf{w}) \tag{2}$$

$\mathbf{w}$ is the conservative flow variable, $\mathbf{F}$ is the flux, $\mathbf{A}$ is the volume of the fluid cell, $\mathbf{u}$ is the structural general displacement and $\mathbf{v}$ is the structural general velocity, $\mathbf{v} = \dot{\mathbf{u}}$, $\mathbf{M}$ is the mass matrix, $\mathbf{f}^{\text{int}}$ is the structural inner force, and $\mathbf{f}^{\text{ext}}$ is the aerodynamic load acting on structures. $(\ )_{,\tau}$ denotes the derivative with respect to non-dimensional time τ, and N_f is the DOFs of the fluid model.

The nonlinear fluid equation can be linearized at a point denoted a convergent steady calculation, in this condition

$$\mathbf{F}(\mathbf{w}_0, \mathbf{u}_0, \mathbf{v}_0) = 0, \quad \mathbf{w}_0 = 0, \quad \mathbf{u}_0 = \mathbf{v}_0 = 0$$

Supposing that $\delta\mathbf{w}$, $\delta\mathbf{u}$, $\delta\mathbf{v}$ are small perturbations around the steady state variables $(\mathbf{w}_0, \mathbf{u}_0, \mathbf{v}_0)$, the perturbation of the state vectors can be written as

$$\mathbf{w} = \mathbf{w}_0 + \delta\mathbf{w}, \quad \dot{\mathbf{w}} = \dot{\mathbf{w}}_0 + \delta\dot{\mathbf{w}}, \quad \mathbf{u} = \mathbf{u}_0 + \delta\mathbf{u}, \quad \mathbf{v} = \mathbf{v}_0 + \delta\mathbf{v}$$

A linearized method is developed by Lesoinne *et al.* [2001], who expand the flow Eq. (1) at $(\mathbf{w}_0, \mathbf{u}_0, \mathbf{v}_0)$ by first order Taylor serials. We can obtain the dynamic linearized equation as following:

$$\mathbf{A}_0(\delta\mathbf{w})_{,\tau} + \mathbf{H}\delta\mathbf{w} + (\mathbf{E} + \mathbf{C})\delta\mathbf{v} + \mathbf{G}\delta\mathbf{u} = 0 \tag{3}$$

where

$$\mathbf{A}_0 = \mathbf{A}(\mathbf{u}_0), \quad \mathbf{H} = \frac{\partial\mathbf{F}}{\partial\mathbf{w}}(\mathbf{w}_0, \mathbf{u}_0, \mathbf{v}_0), \quad \mathbf{C} = \frac{\partial\mathbf{F}}{\partial\mathbf{v}}(\mathbf{w}_0, \mathbf{u}_0, \mathbf{v}_0)$$

$$\mathbf{E} = \frac{\partial\mathbf{A}}{\partial\mathbf{v}}(\mathbf{u}_0)\mathbf{w}_0, \quad \mathbf{G} = \frac{\partial\mathbf{F}}{\partial\mathbf{u}}(\mathbf{w}_0, \mathbf{u}_0, \mathbf{v}_0).$$

Similarly, the structural subsystem can be linearized around an equilibrium state. Equation (2) can be written as

$$\mathbf{M}\delta\dot{\mathbf{v}} + \mathbf{D}_0\delta\mathbf{v} + \mathbf{K}_s\delta\mathbf{u} = \mathbf{P}_0\delta\mathbf{w} \tag{4}$$

where

$$\mathbf{K}_s = \mathbf{K}_0 - \frac{\partial\mathbf{f}^{\text{ext}}}{\partial\mathbf{u}}(\mathbf{w}_0, \mathbf{u}_0), \quad \mathbf{K}_0 = \frac{\partial\mathbf{f}^{\text{int}}}{\partial\mathbf{u}}(\mathbf{u}_0, \mathbf{v}_0),$$

$$\mathbf{D}_0 = \frac{\partial\mathbf{f}^{\text{int}}}{\partial\mathbf{v}}(\mathbf{u}_0, \mathbf{v}_0), \quad \mathbf{P}_0 = \frac{\partial\mathbf{f}^{\text{ext}}}{\partial\mathbf{w}}(\mathbf{w}_0, \mathbf{u}_0)$$

$\mathbf{K}_0$ and $\mathbf{D}_0$ are the structural internal stiffness and damping matrices. $\mathbf{K}_\text{s}$ is an adjusted structural stiffness matrix resulting from the coupled formulation.

To simplify the notation of the linearized equation, $\mathbf{w}$, $\mathbf{u}$, $\mathbf{v}$ are used to represent the perturbation variables $\delta\mathbf{w}$, $\delta\mathbf{u}$, $\delta\mathbf{v}$ respectively. The linearized aeroelastic equations can be written as two coupled matrices

$$\mathbf{A}_0\mathbf{w}_{,\tau} + \mathbf{H}\mathbf{w} + (\mathbf{E}+\mathbf{C})\mathbf{v} + \mathbf{G}\mathbf{u} = \mathbf{0}_{N_f} \tag{5}$$

$$\mathbf{M}\dot{\mathbf{v}} + \mathbf{D}_0\mathbf{v} + \mathbf{K}_s\mathbf{u} = \mathbf{P}_0\mathbf{w}. \tag{6}$$

Equations (5) and (6) are the linearized equations of aeroelastic system. If the grid number of the CFD model is n, the order of Eq. (5) will be $N_f = 4n$ for two-dimensional problems and $N_f = 5n$ for three-dimensional problems. For fluid models, the dimensions of the fluid matrices are too large to numerical simulation, so that ROM techniques are introduced to reduce the linearized fluid equation.

2.2. *Proper orthogonal decomposition method*

POD method provides a basis space that can accurately represent a given data set. The basis can be deemed a low-order model of the original full-order model. For one series of data $\{\mathbf{x}_k\}$, $\mathbf{x}_k \in \mathbf{R}^n$ in the n-dimensional space, m samples of a n-dimensional vectors $\mathbf{x}$ are collected and then the matrix is formed as

$$\mathbf{X} = [\mathbf{x}_1, \mathbf{x}_2, \ldots, \mathbf{x}_m] = \begin{bmatrix} x_{11} & x_{1m} \\ x_{n1} & x_{nm} \end{bmatrix}. \tag{7}$$

The data $\{\mathbf{x}_k\}$ are generated by the drive signals input for the state space equation described in Eq. (5). Then the POD method seeks to find an optimal orthonormal basis, $\mathbf{\Psi}_r = (\Psi_1, \Psi_2, \ldots, \Psi_r)$ (where $r \ll n$) to represent the given data $\{\mathbf{x}_k\}$. Thus, the vector of $\mathbf{x}$ can be expressed as the following expansion:

$$\mathbf{x}^{n\times 1} = \mathbf{\Psi}_r\mathbf{x}_r^{r\times 1}, \tag{8}$$

where $\mathbf{x}_r^{r\times 1}$ are the proper orthogonal coordinate vector and r is the number of DOF of the POD solution.

The POD method was widely applied in structural dynamics [Amsallem *et al.*, 2009] and fluid structural interaction problems [Amsallem, 2010]. The POD theory was complete described by Liang *et al.*, [2002] and we summarize in this paper as following algorithm.

Algorithm 1 (POD method)	
1	Give drive signals to original system and get m samples of a n-dimensional vectors, the matrix formed as $\mathbf{X} = \{\mathbf{x_1}, \ldots, \mathbf{x_m}\}$;
2	Compute correlation matrix $\mathbf{R} = \mathbf{X}^H\mathbf{X} \in \mathbf{R}^{m\times m}$ (H symbol indicates the standard Hermitian operation on a matrix);
3	SVD (singular value decomposition) of $\mathbf{R}, \mathbf{R} = \mathbf{V}\Lambda\mathbf{V}^T$;
4	Compute $\mathbf{\Psi} = \mathbf{X}\mathbf{V}\Lambda \in \mathbf{R}^{n\times \mathrm{snap}}$;
5	Truncating $\mathbf{\Psi}$ to the r-order vector $\mathbf{\Psi}_r = (\Psi_1, \Psi_2, \ldots, \Psi_r) \in \mathbf{R}^{n\times r}$

After getting the low order optimal orthonormal basis $\mathbf{\Psi}_r$, and projecting the full-order Eq. (5) into $\mathbf{\Psi}_r$, we can obtain the reduced system model

$$(\mathbf{w}_r)_{,\tau} + \mathbf{\Psi}_r^T \mathbf{A}_0^{-1} \mathbf{H} \mathbf{\Psi}_r \mathbf{w}_r + \mathbf{\Psi}_r^T \mathbf{A}_0^{-1} (\mathbf{E} + \mathbf{C}) \mathbf{v} + \mathbf{\Psi}_r^T \mathbf{A}_0^{-1} \mathbf{G} \mathbf{u} = \mathbf{0}_r \tag{9}$$

$$\mathbf{M}\dot{\mathbf{v}} + \mathbf{D}_0 \mathbf{v} + \mathbf{K}_s \mathbf{u} = \mathbf{P}_0 \mathbf{\Psi}_r \mathbf{w}_r. \tag{10}$$

The order of the reduced fluid system in Eq. (9) is r, which is much smaller than that of the original system in Eq. (5). POD method is very efficient for large order system, but its accuracy is dependent on the snapshots samples choice. If impulse samples cannot cover all the energy of the original system, some important system dynamics may be missed, which indicates that different operators may lead to different ROM systems.

2.3. *Block Arnoldi method*

The block Arnoldi method is the natural extension of the class Arnoldi process, and it is suitable for the MIMO systems. The block Arnoldi method was applied in many large-scale dynamical systems [Yue and Meerbergen, 2013]. Consider a MIMO system in state-space form

$$\begin{cases} \mathbf{E}\dfrac{d\mathbf{x}(t)}{dt} = \mathbf{A}\mathbf{x}(t) + \mathbf{B}\mathbf{u}(t) \\ \mathbf{y}(t) = \mathbf{C}\mathbf{x}(t). \end{cases} \tag{11}$$

Premutiplying the system by $\mathbf{A}^{-1}$

$$\begin{cases} \mathbf{G}\dfrac{d\mathbf{x}(t)}{dt} = \mathbf{x}(t) + \mathbf{Q}\mathbf{u}(t) \\ \mathbf{y}(t) = \mathbf{C}\mathbf{x}(t) \end{cases} \tag{12}$$

where $\mathbf{G} = \mathbf{A}^{-1}\mathbf{E} \in \mathbf{R}^{n\times n}, \mathbf{Q} = \mathbf{A}^{-1}\mathbf{B} \in \mathbf{R}^{n\times p}, \mathbf{C} \in \mathbf{R}^{m\times n}, \mathbf{u}(t) \in \mathbf{R}^P$ is a $p \times 1$ multi-input variable matrix, and $\mathbf{y}(t) \in \mathbf{R}^m$ is a $m \times 1$ multi-output variable matrix, this system becomes a SISO system when $p = m = 1$. There are two methods for different systems. One is the Arnoldi method for SISO systems and the other is block Arnoldi method for MIMO systems. In the early time, the classic Arnoldi method was developed to reduce the SISO system, and then the block Arnoldi method based on the rth Krylov subspace [Willcox *et al.*, 2002] is applied in a MIMO system.

The MIMO system Eq. (12) corresponding to the rth block Krylov subspace is

$$K_r(\mathbf{G}; \mathbf{Q}) = \mathrm{colspan}\{\mathbf{Q}, \mathbf{G}\mathbf{Q}, \ldots, \mathbf{G}^{r-1}\mathbf{Q}\}$$

Then the block Arnoldi method is used to generate orthonormal basis vectors from this rth order block Krylov subspace, the algorithm is described as following

[Silveira *et al.*, 1999]:

Algorithm 2 (block Arnoldi method)

1 Input matrixes $\mathbf{E}, \mathbf{A}, \mathbf{B}, \mathbf{C}$ and order r;
2 Compute $\mathbf{G} = \mathbf{A}^{-1}\mathbf{E}, \mathbf{Q} = \mathbf{A}^{-1}\mathbf{B}$, and QR factorization $\mathbf{Q}, [\mathbf{V}_1, \mathbf{T}] = \mathbf{qr}(\mathbf{Q})$
3 For $i = 2, \ldots, r+1$
  3.1 calculate $\bar{\mathbf{V}}_i = \mathbf{G} \cdot \mathbf{V}_{i-1}$;
  3.2 for $j = 1, \ldots, i-1$, solve $\mathbf{h}_{j,i-1} = \mathbf{V}_j^T \cdot \mathbf{G} \cdot \mathbf{V}_{i-1}$ and $\overline{\mathbf{V}}_i = \overline{\mathbf{V}}_i - \mathbf{V}_j \cdot \mathbf{h}_{j,i-1}$;
  3.3 QR factorization $\overline{\mathbf{V}}_i$, $[\mathbf{V}_i, \mathbf{h}_{i,i-1}] = \mathbf{qr}(\overline{\mathbf{V}}_i)$;
4 Let $\mathbf{V} = [\mathbf{V_1}, \mathbf{V_2}, \ldots, \mathbf{V}_r]$;
5 Calculate and output $\mathbf{G}_r = \mathbf{V}^T \cdot \mathbf{G} \cdot \mathbf{V}, \mathbf{Q}_r = \mathbf{V}^T \cdot \mathbf{Q}$ and $\mathbf{C}_r = \mathbf{C} \cdot \mathbf{V}$

So the dimensions of reduced system state matrixes are: $\mathbf{G}_r \in \mathbf{R}^{r\times r}, \mathbf{Q}_r \in \mathbf{R}^{r\times p}$ and $\mathbf{C}_r \in \mathbf{R}^{m\times r}$, and then the MIMO system is transformed into a ROM system

$$\begin{cases} \mathbf{G}_r \dfrac{d\tilde{\mathbf{x}}_r(t)}{dt} = \tilde{\mathbf{x}}_r(t) + \mathbf{Q}_r \mathbf{u}(t) \\ \mathbf{y}(t) = \mathbf{C}_r \tilde{\mathbf{x}}_r(t) \end{cases} \tag{13}$$

where $\mathbf{x}(t) = \mathbf{V} \cdot \tilde{\mathbf{x}}_r(t)$, and $\tilde{\mathbf{x}}_r(t)$ has the dimension of $r \times r$. This algorithm is suitable for both SISO and MIMO systems. Different from POD/ROM, the block Arnoldi method is based on the state-space matrixes of original system, so the ROM system is unique when the order of a reduced system is determined. It is very suitable for the linearized aeroelastic system described by Eq. (5), which can also be written as the state-space form.

3. Numerical Simulation

3.1. *Mass–Damper–Spring system case*

A mass–damper–spring system shown in Fig. 1 is considered to assess the effectiveness of the ROM method because it is computationally inexpensive. The same case is also considered using a ROM constructed with the POD technique described by Amsallem [2010].

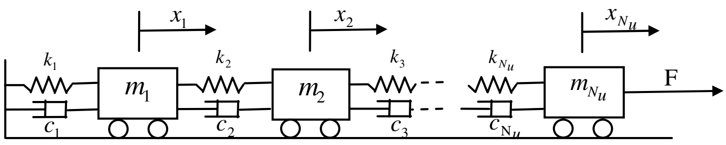

Fig. 1. Mass–damper–spring system with masses m_j, dampers c_j, and spring $k_j, j = 1, \ldots, N_u$.

Each operating point of this mechanical system consists of $3N_u$ parameters corresponding to the $3N_u$ values of the masses m_j, dampers c_j, and spring k_j, $j = 1, \ldots, N_u$. For simplicity, it is assumed that $m_j = m$, $c_j = c$ and $k_j = k$, $j = 1, \ldots, N_u$, so that each operating point of the system is uniquely defined by the three parameters $u = (m, c, k)$ only. Two systems are considered: System 1 is constituted of $N_u^{(1)} = 12$ mass–damper–spring units whereas the system 2 has $N_u^{(2)} = 48$ units. The operating point $u = (0.8, 0.6, 0.7)$ is chosen for both systems. The government equation of this system is

$$\mathbf{M}\ddot{\mathbf{x}} + \mathbf{G}\dot{\mathbf{x}} + \mathbf{K}\mathbf{x} = \mathbf{F} \tag{14}$$

where

$$\mathbf{M} = \begin{bmatrix} 1 & & \\ & \ddots & \\ & & 1 \end{bmatrix} m, \quad \mathbf{G} = \begin{bmatrix} 2 & -1 & & & \\ -1 & 2 & -1 & & \\ & & \ddots & & \\ & & -1 & 2 & -1 \\ & & & -1 & 1 \end{bmatrix} c,$$

$$\mathbf{K} = \begin{bmatrix} 2 & -1 & & & \\ -1 & 2 & -1 & & \\ & & \ddots & & \\ & & -1 & 2 & -1 \\ & & & -1 & 1 \end{bmatrix} k, \quad \mathbf{F} = \begin{bmatrix} 0 \\ \vdots \\ 0 \\ 1 \end{bmatrix} F$$

The second-order system Eq. (18) is first transformed into a first-order system in state-space coordinates, as shown in the following:

$$\begin{aligned} \dot{\mathbf{x}} &= \mathbf{A}\mathbf{x} + \mathbf{B}\mathbf{u} \\ \mathbf{y} &= \mathbf{C}\mathbf{x} + \mathbf{D}\mathbf{u} \end{aligned} \tag{15}$$

where

$$\mathbf{x} = \begin{bmatrix} x_1 \\ \vdots \\ x_n \\ \dot{x}_1 \\ \vdots \\ \dot{x}_n \end{bmatrix}, \quad \mathbf{A} = \begin{bmatrix} \mathbf{0} & \mathbf{I} \\ -\mathbf{M}^{-1}\mathbf{K} & -\mathbf{M}^{-1}\mathbf{G} \end{bmatrix}, \quad \mathbf{B} = \begin{bmatrix} \mathbf{0} \\ \mathbf{M}^{-1} \end{bmatrix}, \quad \mathbf{C} = \begin{bmatrix} 0 \\ \vdots \\ 1 \\ 0 \\ \vdots \\ 0 \end{bmatrix}, \quad \mathbf{D} = [\mathbf{0}]$$

The block Arnoldi method is used to reduce the system's dimension. The system is given a range of $\mathrm{A}_0\sin(\omega t)$ excitation and the signal out of the system will be assumed as $\mathrm{A}_1\sin(\omega t - \Phi)$. Figures 2(a) and 2(b) show the Bode diagrams and Nyquist diagrams of the FOM (full order model) and different order ROMs of

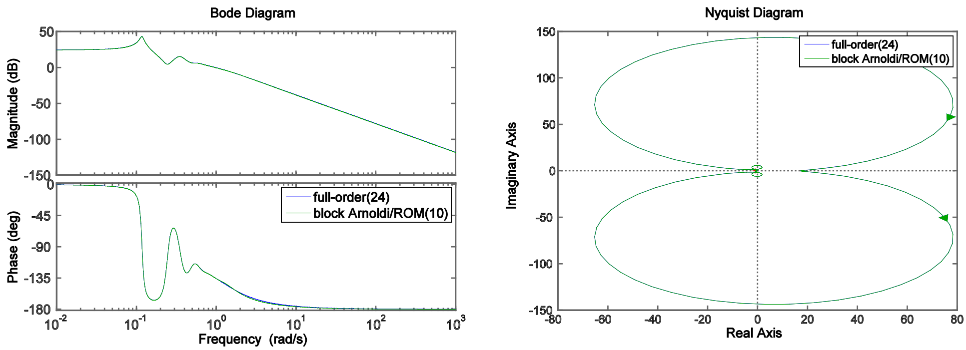

(a)

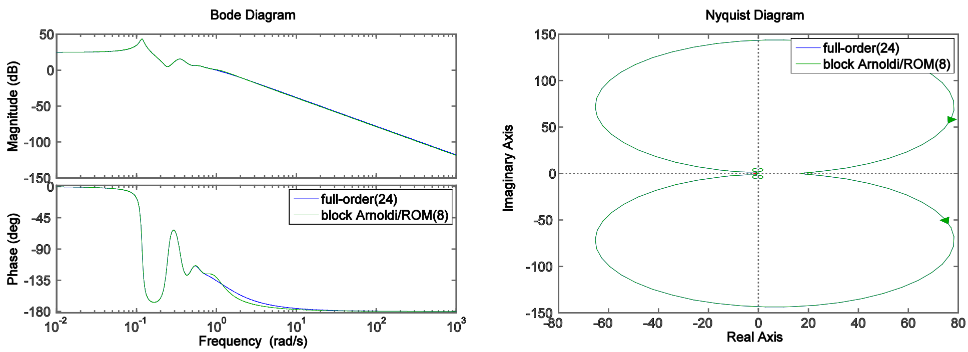

(b)

Fig. 2. Comparison of the frequency responses and Nyquist diagrams of the original system and the ROMs with different size for system 1. (a) Full order system (24) and ROM of size 10. (b) Full order system (24) and ROM of size 8.

system (1). The magnitude of the variable presented in diagram is response gain, which is defined as $20\lg(A_1/A_0)$. The gain and phase shift Φ are a function of frequency. It can be observed that the 10-order ROM is accurate enough for both the low and high frequencies while the 8-order ROM is a little inaccurate. In the Nyquist diagrams, the Nyquist plots are most common used for assessing the stability of a system with feedback. The 10-order and 8-order ROMs have the same stability property with the original system in low and high frequencies.

Various orders' ROMs built by the block Arnoldi method are compared with POD/ROM for system 2. Figures 3 and 4 show the Bode diagrams and Nyquist diagrams of the block Arnoldi/ROM and POD/ROM. In Bode diagrams comparison, for the same 18-order ROM, the phase diagram of Arnoldi/ROM shown in Fig. 3(a) is less accurate than the POD/ROM in Fig. 3(b) in the region of middle frequencies. However, in high excitation frequencies, the 18-order POD/ROM is deviate far away from the full-order diagram while the block Arnoldi/ROM can still

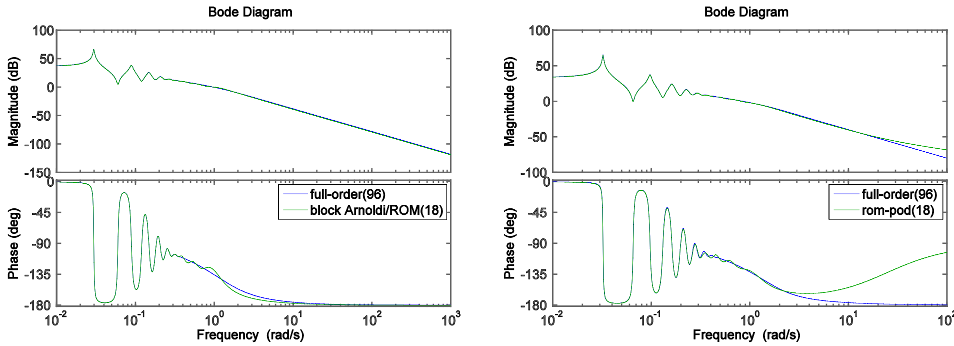

(a) (b)

Fig. 3. Comparison of frequency responses of original and reduced system 2. (a) Full order system (98) and Block Arnoldi method of size 18. (b) Full order system (98) and POD method of size 18

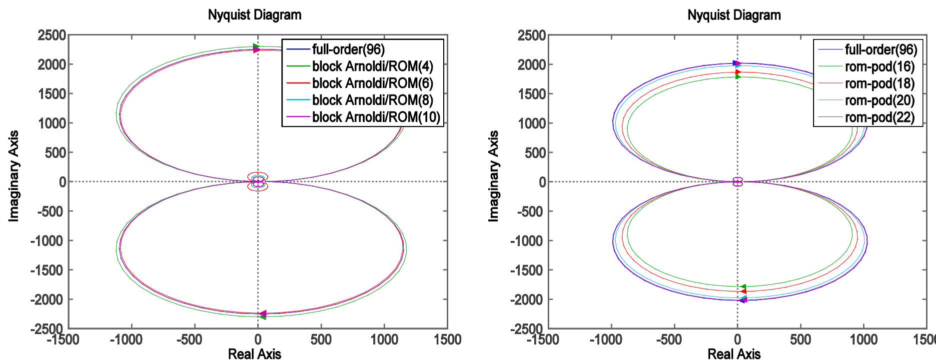

(a) (b)

Fig. 4. Comparison of Nyquist diagrams of system 2. (a) Full order system (96) and Block Arnoldi method of various orders (4, 6, 8 and 10). (b) Full order system (96) and POD method of various orders (16, 18, 20 and 22).

keep the good consistence with the full-order model in both magnitude and phase diagram. In the comparison of Nyquist diagrams from Fig. 4, it can be observed that the 6-order block Arnoldi/ROM is accurate enough while the POD/ROM needs more than 18 vectors to catch the accuracy of the full-order system.

The mass–damper–spring system case demonstrates that the block Arnoldi/ROM provides a good tool for the reduction of a large system in low and high frequencies. It can catch the dominate system behaviors with much lower order than POD/ROM and well maintain the system stability. In the next section, the block Arnoldi/ROM will be constructed for predicting the nonlinear responses of a nonlinear transonic aeroelastic system.

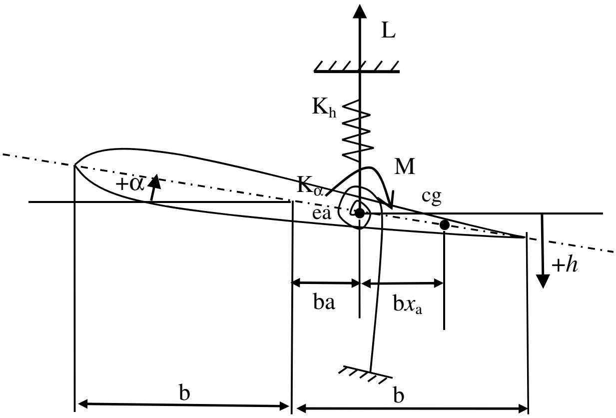

Fig. 5. Aerofoil model with two-degrees (α and h) of freedom.

3.2. *ROMs for nonlinear aeroelastic system*

3.2.1. *Aeroelastic model for pitch-plunge aerofoil*

As shown in Fig. 5, a two-DOF, damped spring mass system allowing for plunging and rotational motion is considered. The torsional motion represents twisting of the wing, and the plunging motion of the section represents bending of the wing along the span. b is semi chord and x_α is the distance between elastic axis and center of gravity, L is the sectional aerodynamic lift (positive up), M is the aerodynamic moment about the center of gravity (positive nose up), K_h and K_α are bending and torsional spring stiffness, and h and α are the plunging coordinate (positive down) and the angle of attack (in radians). The equation of motion for the system can be written by considering sum of all forces and moments acting on the aerofoil center of gravity.

Based on Lagrange equation, the dynamic equations of the aeroelastic system can be written as

$$\begin{aligned} m\ddot{h} + S_\alpha\ddot{\alpha} + K_h h &= -L \\ S_\alpha\ddot{h} + I_\alpha\ddot{\alpha} + K_\alpha\alpha &= M \end{aligned} \tag{16}$$

where

$$S_\alpha = \int_0^{2b} r dm = m x_\alpha b, \quad L = \rho_\infty^2 b C_L$$

$$I_\alpha = \int_0^{2b} r^2 dm = m r_\alpha^2 b^2, \quad M = 2\rho_\infty^2 b^2 C_M$$

r_α^2 is radius of gyration per half cord (squared).

By defining $\tau = tU/b$, $\dot{(\,)}$ indicates a differentiation with respect to t and $(\,)'$ indicates a differentiation with respect to τ, so that $\dot{(\,)} = U/b(\,)'$. Then Eq. (17) can be written in non-dimensional form [Da Ronch *et al.*, 2012].

$$\begin{aligned} \xi_1'' + x_\alpha \alpha'' + \left(\frac{\bar{\omega}}{U^*}\right)^2 \xi_1 &= -\frac{1}{\pi\mu} C_L(\tau) \\ x_\alpha \xi_1'' + r_a^2 \alpha'' + \left(\frac{r_a}{U^*}\right)^2 \alpha &= \frac{2}{\pi\mu} C_m(\tau) \end{aligned} \tag{17}$$

where $\xi_1 = h/b$, U^* is reduced velocity $U^* = U/(b \cdot \omega_\alpha)$, μ is mass ratio $\mu = m/\pi\rho b^2$, and $\bar{\omega} = \omega_h/\omega_\alpha$. The system dynamic Eq. (17) can be written in matrix form as

$$\mathbf{M} \cdot \ddot{\boldsymbol{\xi}} + \mathbf{K} \cdot \boldsymbol{\xi} = \mathbf{F} \tag{18}$$

where

$$\boldsymbol{\xi} = \begin{Bmatrix} \xi_1 \\ \xi_2 \end{Bmatrix} = \begin{Bmatrix} h/b \\ \alpha \end{Bmatrix}, \quad \mathbf{M} = \begin{bmatrix} 1 & x_\alpha \\ x_\alpha & r_\alpha^2 \end{bmatrix},$$

$$\mathbf{K} = \begin{bmatrix} (\bar{\omega}/U^*)^2 & 0 \\ 0 & (r_\alpha/U^*)^2 \end{bmatrix}, \quad \mathbf{F} = \frac{1}{\pi\mu} \begin{Bmatrix} -C_L \\ 2C_M \end{Bmatrix}.$$

3.2.2. *Linearization model validation*

In order to accurately predict the aeroelastic responses, the full-order linearized unsteady aerodynamics C_L and C_M should be validated first. The Euler equation is discretized by the second-order Van Leer scheme on the 80×30 O-type structural meshes. NACA0012 aerofoil with unsteady plunging motion was analyzed in this subsection. Meshes of the flow field are shown in Fig. 6. The full-order linearized flow equation DOFs is $N_{\mathrm{f}} = 4 \times 80 \times 30 = 9600$. The initial flow condition is $\mathrm{Ma} = 0.70$,

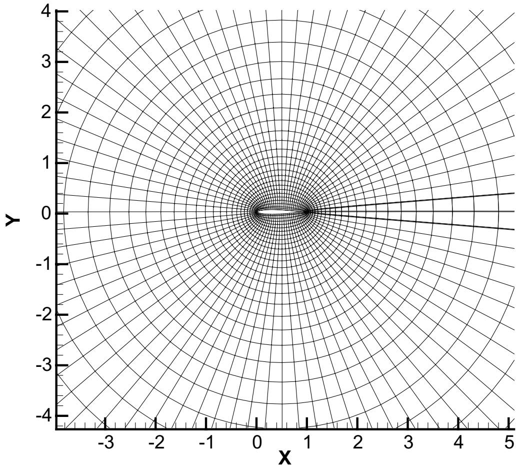

Fig. 6. Computational domain for NACA0012 aerofoil.

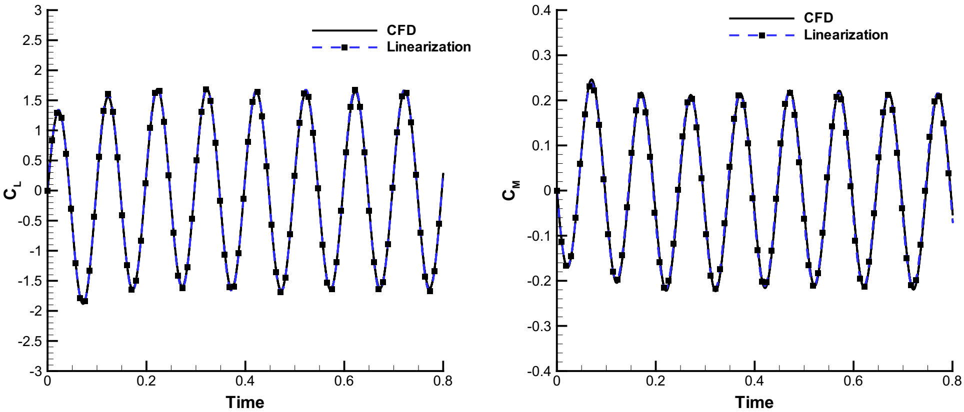

(a) (b)

Fig. 7. Comparison the responses of the linearized model and nonlinear CFD model under prescribed oscillation of a NACA0012 aerofoil at condition of $Ma = 0.70$, $\alpha = 0°$, $h/b = 0.01\sin(\omega t)$, $\omega = 20\pi$. (a) Lift coefficient response with time and (b) moment coefficient response with time.

$\alpha = 0°$ and the aerofoil oscillates as $h/b = 0.01\sin(\omega t)$, $\omega = 20\pi$. Figures 7(a) and 7(b) show the time responses of the unsteady aerodynamic loads at a time step of $dt = 2\pi/20000s$. The responses are predicted by the dynamic linearized model based on CFD and nonlinear unsteady CFD, respectively. The good agreement of the two models indicates that the dynamic linearized model has near the same accuracy as the nonlinear CFD model at small perturbation.

In order to analyze the stability of the aeroelastic system, Eq. (18) must be coupled with Eq. (1) or Eq. (5). So next we will analyze the free responses of the couple system after a small disturbance in pitching motion is given. The parameters for NACA0012 structural model are shown in Table 1. This test case corresponds the heave case was described by Badcock *et al.* [2004]. At the condition of $Ma = 0.5$, $U^* = 1.0$, different free responses including Plunge, Angle of attack and force coefficient are shown in Figs. 8(a)–8(d). From the time responses described in Fig. 8, the system is asymptotically stable. The tendency and amplitude of different models are very close except a little fluctuation in Fig. 8(b) corresponding angle of attack. So the linearized model based on CFD solver is accurate enough for a small perturbation to the system. After validating the accuracy of aerofoil prescribed oscillation and free aeroelastic responses by the linearized model, the model will be used to construct ROMs in next section.

Table 1. Inertial parameters for NACA0012 aeroelastic model.

Parameter	$\bar{\omega}$	μ	a	x_α	r_α
Value	0.342	100	−0.2	0.2	0.539

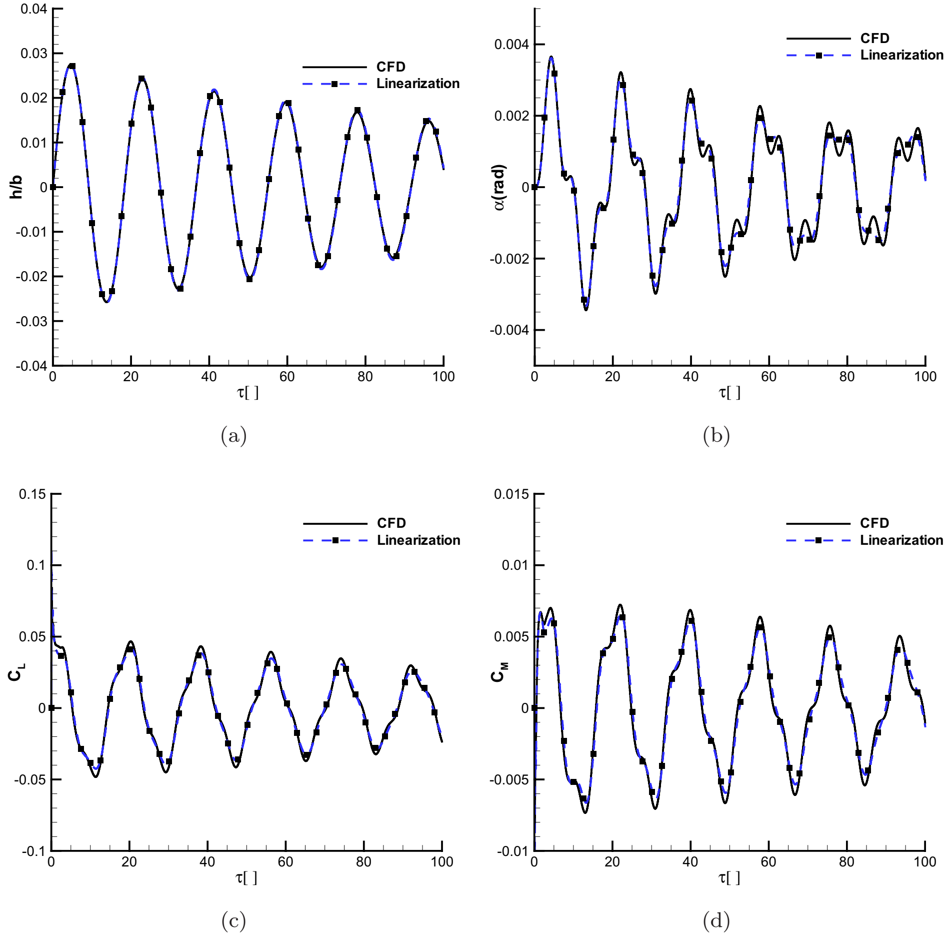

Fig. 8. Comparison the free responses of the linearized model and nonlinear CFD model at the initial condition of $Ma = 0.5$, $U^* = 1.0$, $\boldsymbol{v}_1 = 0.01$ ($t = 0$). (a) Plunge response with time, (b) angle of attack response with time, (c) lift coefficient response with time and (d) moment coefficient response with time.

3.2.3. *Aeroelastic responses based on ROM*

In the same flow condition above, at the base of linearization model, the POD snapshots are calculated in time domain with the time step of 5×10^{-3} s. And taking 800 snapshots samples of the resulting uncoupled fluid response by given that 2 displacement and 2 velocity inputs. Based on the snapshots samples, we reduce the full-order linearized model to a 50-order and a 20-order model by POD/ROM. And then we reduce the linearized model to an 8-order model directly through Eq. (5) by block Arnoldi/ROM. The aeroelastic responses predicted by different models were presented in Figs. 9(a)–9(d). It is obviously seen that the aeroelastic responses of the 8-order block Arnoldi/ROM are as nearly the same accurate as those of

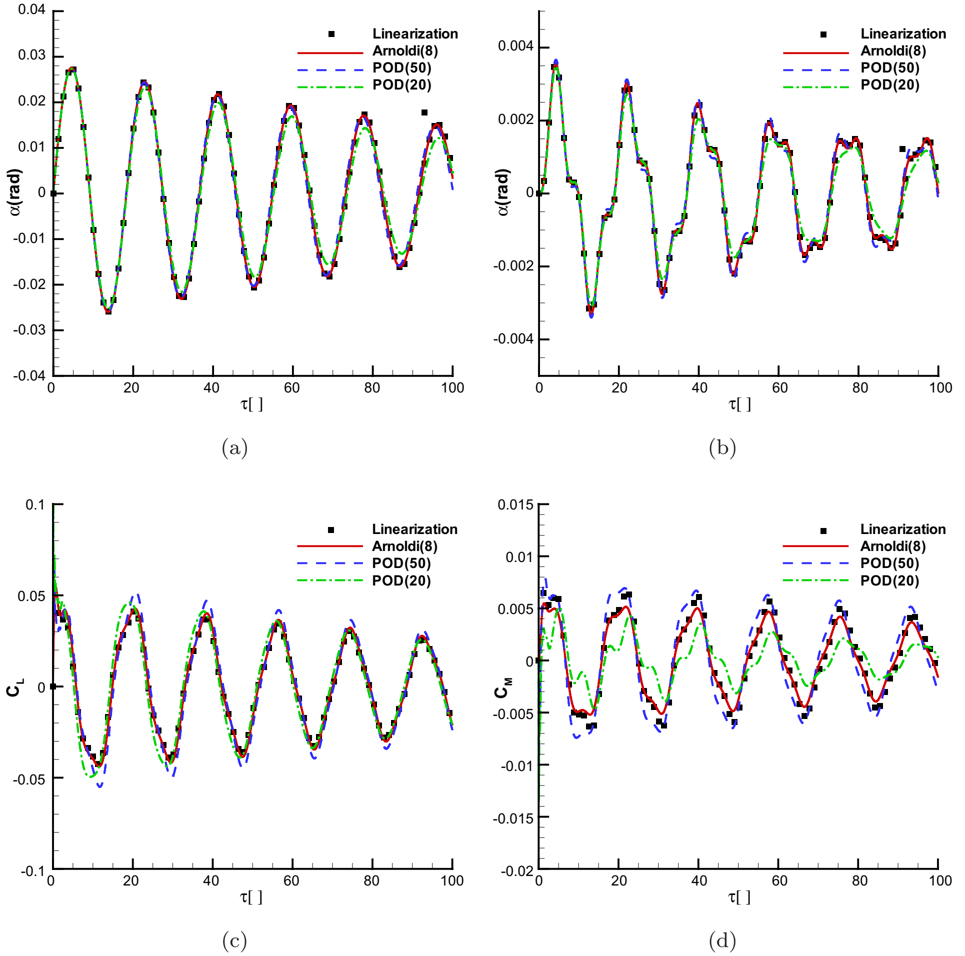

Fig. 9. Comparison the free responses of the linearized model and different ROMs at the initial condition of $Ma = 0.5$, $U^* = 1.0$, $v_1 = 0.01\,(t = 0)$. (a) Plunge, (b) angle of attack, (c) lift coefficient and (d) moment coefficient.

the full-order linearized model. As the POD method is sensitive to the choice of snapshots and difficult to produce snapshots which contain all the energy inspired by drive signal, even the 50-order POD/ROM has not good accuracy with the 8-order Arnoldi/ROM. The lower order models are expected in control design and optimization design. At the beginning, different models' curves are very consistent, while with the increase of the time, different ROM models' results gradually slightly deviate from the full order model.

From the displacement response results shown in Figs. 9(a) and 9(b), the difference between the 8-order Arnoldi/ROM and 50-order POD/ROM calculations is small. However, from the force and moment responses in Figs. 9(c) and 9(d), the 50-order (blue dashed line) and 20-order (green dashdot line) POD results show obvious deviation with the full-order linearization results. While the results calculated by the 8-order block Arnoldi/ROM (black solid line) keep a good tendency with the full order model. These analyses indicate that the block Arnoldi/ROM with less order can well keep the stability of the system characteristic and does not appear large deviation with the full-order system in time-varying phenomena. However, a higher number order POD/ROM is required to maintain the tendency and accuracy.

3.2.4. *Flutter boundary prediction*

To find a flutter point at a given Mach number, different reduced velocity U^* should be tested through coupling simulations. Figs. 10(a)–10(c) are the responses

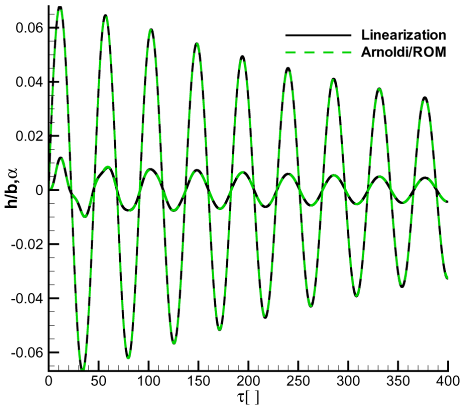

(a)

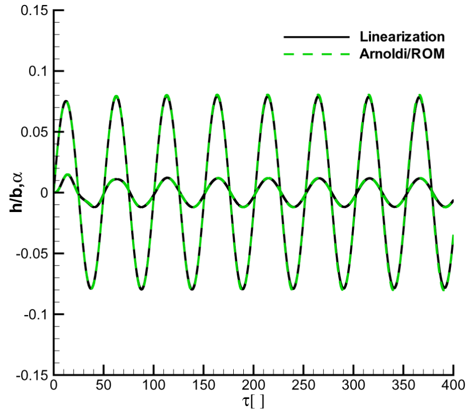

(b)

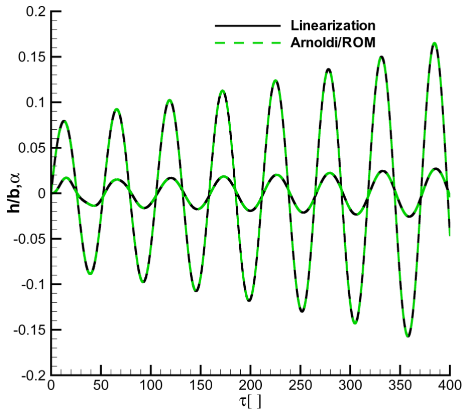

(c)

Fig. 10. Responses comparison at different reduced velocity in Mach 0.8. (a) $U^* = 2.8$, amplitude damp with time indicates stable situation. (b) $U^* = 3.23$, amplitude unchanged with time indicates neutral situation. (c) $U^* = 3.5$, amplitude diverge with time indicates unstable situation.

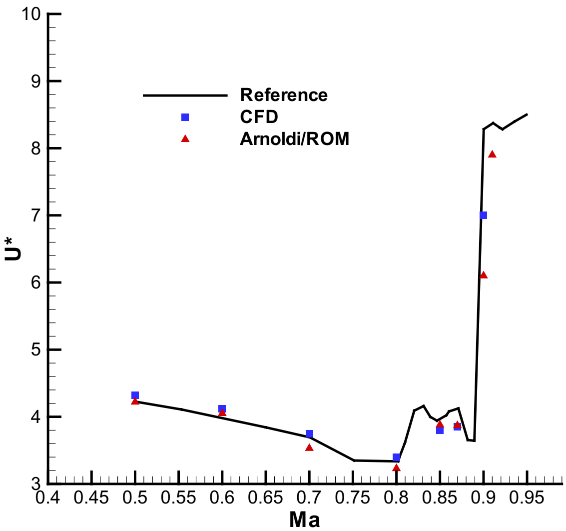

Fig. 11. Flutter boundary prediction of NACA0012 aeroelastic model by block Arnoldi/ROM, CFD/CSD coupling simulation and reference [Badcock *et al.*, 2004].

comparison at different reduced velocity at Mach 0.8. As shown in Fig. 10(a) at $U^* = 2.8$, the pitching and plunging amplitudes damp with time, indicating that the aeroelastic system is stable at this condition. Figure 10(b) is the flutter point responses at $U^* = 3.23$ and Fig. 10(c) shows the system is unstable because pitching and plunging responses diverge with time.

At last, we will apply the block Arnoldi/ROM to predict the flutter boundary of the NACA0012 aeroelastic model between Mach numbers of 0.5 and 0.91. The transonic effects are included in this Mach range and the time step is 0.01 s. The order of the selected Arnoldi/ROM is 44 (40 fluid Dofs and 4 structural Dofs) which is much smaller than the full order model with 9604 (9600 fluid Dofs and 4 structural Dofs). The comparisons of the flutter boundary predicted by CFD, Arnoldi/ROM and reference results [Badcock *et al.*, 2004] are shown in Fig. 11. It can be noted that our CFD solver and Arnoldi/ROM can well compare with the reference results base on hopf bifurcation calculations. The results are also very sensitive to the Mach numbers in transonic region (about $Ma = 0.8 - 0.91$). So it is tedious and time consuming to find the flutter boundary in this region by a CFD/CSD couple solver. However, the use of low order model produced by block Arnoldi/ROM just needs several seconds to judge the system stable or not. The block Arnoldi/ROM provides a good tool to aeroelastic system stability analysis.

4. Conclusion

A reduced order modeling based on the block Arnoldi method for nonlinear MIMO transonic aeroelastic systems has been investigated. A simple mass–damper–spring system and a two-DOF transonic nonlinear aerofoil aeroelastic system were used to demonstrate the efficiency and accuracy of this method. POD/ROM is also tested to compare with block Arnoldi/ROM. In the block Arnoldi method, the construction of the basis vectors only requires the matrixes of the state-space equations of the full-order model, while the POD/ROM is obtained from the system snapshots which may be sensitive to the choice of drive signals or frequencies. The mass–damper–spring case shows that the low order system produced by the block Arnoldi method can well keep the dynamic property with the original system in low and high frequencies while the POD/ROM has some deviation in high frequencies. At last, the flutter boundary of NACA0012 aeroelastic system was quickly obtained through the block Arnoldi/ROM and well compared with the CFD/CSD coupling method and reference results. The block Arnoldi/ROM provides a good tool to analyze MIMO nonlinear transonic aeroelastic system's stability. With the low order model produced by Arnoldi/ROM, it is easy to couple structural equations and control models for active control law design.

Acknowledgments

This work was partially' supported by the National Basic Research Program of China (2013CB03570202), the National Natural Science Foundation of China (11272005, 11472206), and the Funds for the Central Universities (xjj2014135).

References

Amabili, M., Sarkar, A. and Païdoussis, M. [2003] "Reduced-order models for nonlinear vibrations of cylindrical shells via the proper orthogonal decomposition method," *Journal of Fluids and Structures* **18**(2), 227–250.

Amsallem, D. [2010] "Interpolation on manifolds of CFD-based fluid and finite element-based structural reduced-order models for on-line aeroelastic predictions," Ph.D. thesis, Stanford University, State of California.

Amsallem, D., Cortial, J., Carlberg, K. and Farhat, C. [2009] "A method for interpolating on manifolds structural dynamics reduced-order models," *International Journal for Numerical Methods in Engineering* **80**(9), 1241–1258.

Badcock, K. J., Woodgate, M. A. and Richards, B. E. [2004] "Hopf bifurcation calculations for a symmetric airfoil in transonic flow," *AIAA Journal* **42**(5), 883–892.

Batra, R., Porfiri, M. and Spinello, D. [2008] "Reduced-order models for microelectromechanical rectangular and circular plates incorporating the Casimir force," *International Journal of Solids and Structures* **45**(11), 3558–3583.

Besselink, B., Tabak, U., Lutowska, A., van de Wouw, N., Nijmeijer, H., Rixen, D., Hochstenbach, M. and Schilders, W. [2013] "A comparison of model reduction techniques from structural dynamics, numerical mathematics and systems and control," *Journal of Sound and Vibration* **332**(19), 4403–4422.

Bui, T. Q. and Nguyen, M. N. [2011] "Eigenvalue analysis of thin plate with complicated shapes by a novel mesh-free method," *International Journal of Applied Mechanics* **3**(01), 21–46.

Chen, G., Li, Y. M. and Yan, G. R. [2010] "A nonliner POD reduced order for limit cycle oscillation prediction," *Science China Physics, Mechanics and Astronomy* **53**(7), 1325–1332.

Chen, G., Li, Y. M. and Yan, G. R. [2011] "Limit cycle oscillation prediction and control design method for aeroelastic system based on new nonlinear reduced order model," *International Journal of Computational Methods* **8**(01), 77–90.

Chen, G., Sun, J. and Li, Y. M. [2012] "Active flutter suppression control law design method based on balanced proper orthogonal decomposition reduced order model," *Nonlinear Dynamics* **70**(1), 1–12.

Chen, G., Wang, X. and Li, Y. M. [2014] "A reduced-order-model-based multiple-in multiple-out gust alleviation control law design method in transonic flow," *Science China Technological Sciences* **57**(2), 368–378.

Da Ronch, A., Badcock, K. J., Wang, Y., Wynn, A. and Palacios, R. [2012] "Nonlinear model reduction for flexible aircraft control design," *AIAA Atmospheric Flight Mechanics Conference*, Minneapolis, Minnesota, pp. 13–16.

Florea, R., Hall, K. C. and Dowell, E. H. [2000] "Eigenmode analysis and reduced-order modeling of unsteady transonic potential flow around airfoils," *Journal of Aircraft* **37**(3), 454–462.

Griffith, B. E., Luo, X., McQueen, D. M. and Peskin, C. S. [2009] "Simulating the fluid dynamics of natural and prosthetic heart valves using the immersed boundary method," *International Journal of Applied Mechanics* **1**(01), 137–177.

Kergourlay, G., Balmes, E. and Clouteau, D. [2001] "Model reduction for efficient FEM/BEM coupling," *Proceedings of the International Seminar on Modal Analysis*, Vol. 3, KU Leuven, pp. 1167–1174.

Kerschen, G., Golinval, J.-C., Vakakis, A. F. and Bergman, L. A. [2005] "The method of proper orthogonal decomposition for dynamical characterization and order reduction of mechanical systems: An overview," *Nonlinear Dynamics* **41**(1–3), 147–169.

Lantz, J., Renner, J. and Karlsson, M. [2011] "Wall shear stress in a subject specific human aorta — influence of fluid-structure interaction," *International Journal of Applied Mechanics* **3**(04), 759–778.

Lesoinne, M., Sarkis, M., Hetmaniuk, U. and Farhat, C. [2001] "A linearized method for the frequency analysis of three-dimensional fluid/structure interaction problems in all flow regimes," *Computer Methods in Applied Mechanics and Engineering* **190**(24), 3121–3146.

Li, K., Zhang, J. and Mei, G. [2012] "Aerothermoelastic model of panel flutter with consideration of the history effects of aerodynamic heating," *International Journal of Applied Mechanics* **4**(03).

Liang, Y. C., Lee, H. P., Lim, S. P., Lin, W. Z., Lee, K. H. and Wu, C. G. [2002] "Proper orthogonal decomposition and its applications — Part I: Theory," *Journal of Sound and Vibration* **252**(3), 527–544.

Lucia, D. J., Beran, P. S. and Silva, W. A. [2004] "Reduced-order modeling: New approaches for computational physics," *Progress in Aerospace Sciences* **40**(1), 51–117.

Puri, R. S. and Morrey, D. [2011] "A Krylov–Arnoldi reduced order modelling framework for efficient, fully coupled, structural–acoustic optimization," *Structural and Multidisciplinary Optimization* **43**(4), 495–517.

Rumpler, R., Göransson, P. and Deü, J. F. [2014] "A finite element approach combining a reduced — order system, Padé approximants, and an adaptive frequency windowing for fast multi-frequency solution of poro-acoustic problems," *International Journal for Numerical Methods in Engineering* **97**(10), 759–784.

Silveira, L. M., Kamon, M., Elfadel, I. and White, J. [1999] "A coordinate-transformed Arnoldi algorithm for generating guaranteed stable reduced-order models of RLC circuits," *Computer Methods in Applied Mechanics and Engineering* **169**(3), 377–389.

Steindl, A. and Troger, H. [2001] "Methods for dimension reduction and their application in nonlinear dynamics," *International Journal of Solids and Structures* **38**(10), 2131–2147.

Tan, F., Torii, R., Borghi, A., Mohiaddin, R., Wood, N. and Xu, X. [2009] "Fluid-structure interaction analysis of wall stress and flow patterns in a thoracic aortic aneurysm," *International Journal of Applied Mechanics* **1**(01), 179–199.

Willcox, K., Peraire, J. and White, J. [2002] "An Arnoldi approach for generation of reduced-order models for turbomachinery," *Computers and Fluids* **31**(3), 369–389.

Xu, F., Hu, H., Potier-Ferry, M. and Belouettar, S. [2014] "Bridging techniques in a multi-scale modeling of pattern formation," *International Journal of Solids and Structures* **51**(18), 3119–3134.

Yue, Y. and Meerbergen, K. [2013] "Parametric model order reduction of damped mechanical systems via the block Arnoldi process," *Applied Mathematics Letters* **26**(6), 643–648.